Proceedings of the ASME 2024 19th International Manufacturing Science and Engineering Conference MSEC2024
June 17-21, 2024, Knoxville, Tennessee

MSEC2024-124723

IN SITU OBSERVATIONS OF SHEAR LOCALIZATION AND FRACTURE IN MACHINING

Shwetabh Yadav[1,*], Harshit Chawla[2], Dinakar Sagapuram[2],

[1]Indian Institute of Technology Hyderabad, India
[2]Texas A&M University, College Station, TX

ABSTRACT

Using direct high-speed imaging, we study the transition between different chip formation modes, and the underlying mechanics, in machining of ductile metals. Three distinct chip formation modes — continuous chip, shear-localized chip, and fragmented chip — are effected in a same material system by varying the cutting speed. It is shown using direct observations that shear-localized chip formation is characterized by shear band nucleation at the tool tip and its propagation towards the free surface, which is then followed by plastic slip along the band without fracture. The transition from shear-localized chip to fragmented chip with increasing cutting speed is triggered by crack initiation at the free surface and propagation towards the tool tip. The extent to which crack travels towards the tool determines whether the chip is partially fragmented or fully fragmented (discontinuous). It is shown that shear localization precedes fracture and controls the crack path in fragmented chip formation. Dynamic strain and strain-rate fields underlying the each chip formation mode are quantified through image correlation analysis of high-speed images. Implications for using machining as an experimental tool for fundamental studies of localization and shear fracture in ductile metals are also discussed.

Keywords: metal cutting, shear banding, discontinuous chips, imaging

1. INTRODUCTION AND BACKGROUND

Chip formation in metal cutting is an unconfined plastic deformation process that is accompanied by large strains (1 – 10), high strain rates (up to 10^5 per second), combined with adiabatic temperature rise in the deformation zone [1, 2]. In this regard, cutting differs from other metal plastic deformation processes such as forming in two main aspects: (1) unconstrained plastic flow at the workpiece/chip free surface, which makes cutting a free-boundary value problem; and (2) metal plasticity under extreme strain and strain rate conditions that fall outside the range of most forming processes. It is for this reason that steady-state plastic flow is an exception rather than the norm in metal cutting and this deviation from the steady state triggers a rich variety of chip formation modes in addition to the well-known continuous chip. These for example include the so-called Type 1 chip in soft and highly strain-hardening metals, which is characterized by unusually large chip thickness ratio (up to 15) and an inherently unsteady sinuous flow [3]; the segmented chip with periodic variations in the chip thickness that occurs when cutting under small or negative rake angles [4, 5]; the saw-tooth or shear-localized chip which arises as a result of periodic shear banding and is most prominent in metals with low thermal conductivity/diffusivity [6–9]; and the fully discontinuous chip (i.e., broken chips) often seen when cutting metals with limited ductility [10, 11].

While the specific mode of chip formation is governed to a large extent by the workpiece material properties, there are several instances where transitions between different chip formation modes can occur within a same material system upon varying the cutting conditions. One such case, which is the focus of this paper, is the transition from continuous chip to shear-localized chip, and its subsequent transformation into a fully fragmented chip, upon increasing the cutting speed. Several metals have been reported in the literature to exhibit this phenomenon, with titanium, steels and nickel-based superalloys being the most studied examples [6, 12–16]. In these materials, as the cutting speed is increased, the continuous chip is replaced by a shear-localized chip with periodic shear bands. The latter has a characteristic saw-tooth appearance and is characterized by a highly inhomogeneous deformation, with shear bands showing a highly concentrated plastic flow (shear strains up to 50 are common within shear bands), while large regions (segments) in between the bands are deformed to only small strains [17]. In some cases, partial material separation in the form of a crack is also observed along the shear bands [15, 16]. A second transition — from shear-localized to a fragmented chip — occurs with further increase in speed. In this regime, cutting results in formation of individual and completely broken segments [12]. The "critical" cutting speeds at which these transitions occur are known to primarily depend on the material and its metallurgical condition.

*Corresponding author: shwetabh@ce.iith.ac.in

Most attempts to understand the mechanism of shear-localized chip formation have relied on post-mortem observations of the chip morphology or the quick-stop method, wherein the tool and workpiece are quickly disengaged to "freeze" the cutting process. Based on these studies, it has been suggested that strain localization first begins at the tool tip which then propagates from tool tip to the free surface [15, 18, 19]. However, entirely opposite points of view also exist, for example those by Shaw [16], Usui [20] and Nakayama [4], who suggest that initiation of a small crack at the workpiece/chip surface gives rise to concentrated slip or localization along the line connecting surface crack and the tool tip. Unfortunately, quick-stop methods are not capable of resolving temporal details, not to mention that they can also introduce their own artefacts due to rapid unloading of the material. Therefore, whether fracture precedes shear localization or vice versa is still not clear. Even less clarity surrounds the issue of fully fragmented or discontinuous chip, with some studies suggesting the initiation of cracks near the tool edge [21, 22] while other evidence pointing towards crack initiation at, and propagation, from the free surface [15]. It therefore appears that direct *in situ* observations of the chip formation process would be valuable for capturing the shear band/crack dynamics and how interaction between both the processes influences the overall chip formation mode. However, given the extremely small spatial and temporal scales associated with shear bands and cracks, it is important that such observations are made at high spatial and temporal resolution.

Recent advancements in high-speed imaging and image analysis techniques such as digital image correlation (DIC) and particle image velocimetry (PIV) have enabled direct *in situ* measurements of chip formation process at sufficiently high spatial and temporal resolution required for such studies [5]. For example, in our earlier studies, we have used *in situ* imaging, in combination with a low melting point alloy as a model system, to study the dynamics of shear-localized chip formation and resolve key aspects of shear band nucleation and growth [23–25]. These studies, for instance, have suggested the existence of a critical shear stress for shear band nucleation and revealed similarities between localized plastic flow around a band and the classical boundary layer phenomenon in viscous fluids. This paper builds on our earlier work with an expanded focus on understanding the transition between shear-localized chip and fragmented chip at higher cutting speeds. Simultaneous *in situ* imaging and force measurements were used in the study for this purpose. The main contribution of the paper lies in conclusively showing that shear localization is a *precursor* to fracture, and not the opposite. From a phenomenological standpoint, the study has also revealed several interesting aspects of (shear) fracture during chip formation, including the crack nucleation site and crack propagation dynamics.

2. EXPERIMENTAL

Wood's alloy, a low melting-point (T_m = 70 °C) bismuth-based eutectic alloy, was used as a model material system to study transitions in the chip formation mode upon increase in the cutting speed. The choice of this alloy was motivated by our recent discovery [24] that low T_m eutectic alloys exhibit a transition from continuous chip to shear-localized chip at cutting speeds (0.01-10 mm/s) that are multiple orders of magnitude lower than the typical cutting speeds (> 1 m/s) at which shear localization is typically observed in engineering alloys such as titanium and steels. This offers an interesting opportunity to directly observe the transitions in the chip formation mode and study in detail basic aspects related to dynamics of shear band and crack formation. Furthermore, the quasi-static plastic deformation response of low T_m eutectic alloys — characterized by high strain-rate sensitivity and negligible strain hardening — is akin to the dynamic response of common alloys at high strain rates. This allows generalization of observations and results from the study to other materials that exhibit similar transitions in the chip formation mode at higher cutting speeds.

Wood's alloy with a nominal composition of 50% Bi, 26.7% Pb, 13.3% Sn and 10% Cd (by weight) was obtained from Belmont Metals Inc. (Brooklyn, NY) in the form of an ingot and cast into rectangular plate samples (75 mm × 25 mm × 2 mm) by preheating the metal to 200 °C and pouring it into a rectangular-shaped aluminum molds, see Ref. [24] for details. Orthogonal cutting experiments were carried out in a linear planing configuration using a freshly ground high-speed steel tool with a 0° rake angle and an edge radius of < 10 μm; the average surface roughness (R_a) of the rake face was about 0.4 μm. The depth of cut (t_0) was kept constant at 250 μm, the cutting width (b) was 2 mm, and the cutting speed (V_0) was varied over three orders of magnitude from 0.01 mm/s to 10 mm/s. As shall be seen later, this V_0 range covers the full spectrum of chip formation modes from continuous to shear-localized to fully fragmented chip.

To directly observe the chip formation process *in situ*, a high-speed camera (PCO Dimax HS4) coupled to a 10X objective lens was used in the study. The orthogonal cutting setup is such that the cutting tool is fixed (stationary), with the workpiece sample moving against the tool with a specified V_0; therefore, in this configuration, the plastic deformation zone is stationary with respect to the observer (see Fig. 1). Another important feature of our setup is the use of a transparent sapphire plate to lightly constrain the workpiece side-surface that is being imaged. This was done to suppress out-of-plane material flow and to ensure that the observations made on the sample surface are representative of the bulk response. High-speed images were captured at a spatial resolution of 0.95 μm per pixel over a $\sim 1.5 \times 1.5$ mm^2 field of view, at frame rates in the range of 1-10 kHz, depending on V_0.

To obtain quantitative full-field plastic strain and strain-rate data, the high-speed images of the cutting zone were analyzed using a digital image correlation technique called Particle Image Velocimetry (PIV) [26]. In this method, features on the material surface — introduced artificially before the start of the experiment — are tracked during the cutting process to obtain the instantaneous displacement field in the deformation zone. The equivalent plastic strain rate ($\dot{\varepsilon}$) and strain (ε) fields were calculated from the displacement field using the Green strain tensor formulation for plane-strain, see Refs. [24, 27] for a detailed description of the algorithm and its application to the cutting process. The high spatial and temporal resolution of the imaging setup, coupled with quantitative PIV analysis, allowed us the track shear band/crack initiation events, as well of their subsequent evolution. In all the experiments, cutting force components parallel and perpendicu-

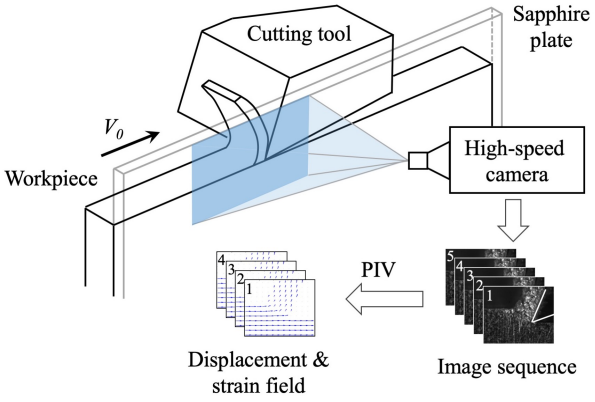

FIGURE 1: SCHEMATIC OF THE CUTTING EXPERIMENTAL SETUP USED IN THE STUDY FOR *IN SITU* IMAGING AND PIV ANALYSIS.

lar to V_0 direction were also measured using a piezoelectric force sensor (Kistler 9129AA) mounted directly under the tool; this enabled direct correlations to be made between various stages of the chip formation process, as observed from high-speed images, and the macroscopic force response on the cutting tool.

3. RESULTS

Direct *in situ* observations of chip formation over a range of cutting speeds (from 0.01 to 10 mm/s) have enabled comprehensive characterization of the mechanics of three distinct chip formation modes — continuous, shear-localized and fragmented chip — and underlying transitions as the cutting speed is increased.

3.1 Continuous chip

Figure 2 shows the continuous chip formation mode that was observed at a very low cutting speed of 0.05 mm/s. Figures 2(A) and (B) respectively are the grid and equivalent plastic strain field maps, as obtained using the PIV analysis, while Fig. 2(C) shows the forces acting on the tool; F_1 and F_2 are the forces along and normal to the V_0 direction, respectively. The classical smooth ribbon-type chip is evident, characterized by uniform thickness and deformation. The uniformity of deformation, for instance, can be seen from the grid map (Fig. 2(A)) where the deformed rhomboid shape of the grid elements is nearly uniform throughout the chip. This is also evident from the uniform strain distribution along the length of the chip in Fig. 2(B). The average strain in the chip is about 1.2, which is close to the the value of 1.1 calculated based on steady-state shear along a single shear plane OO' [1]. The steady-state nature of chip formation is also reflected in the force profiles (Fig. 2(C)), which show less than 10% variation around their mean during the entire duration of the cut. The shear stress along the shear plane OO' was estimated using the Merchant's analysis [28] using the average F_1 and F_2 values and the shear plane angle ($\phi \sim 40°$). The estimated shear stress of 55 MPa compares well with the equivalent shear flow stress of ~ 60 MPa for the Wood's alloy obtained from uniaxial compression experiments [24, 25].

3.2 Shear-localized chip

Increase in V_0 to > 0.6 mm/s results in a transition from continuous chip to shear-localized chip that is characterized by saw-tooth

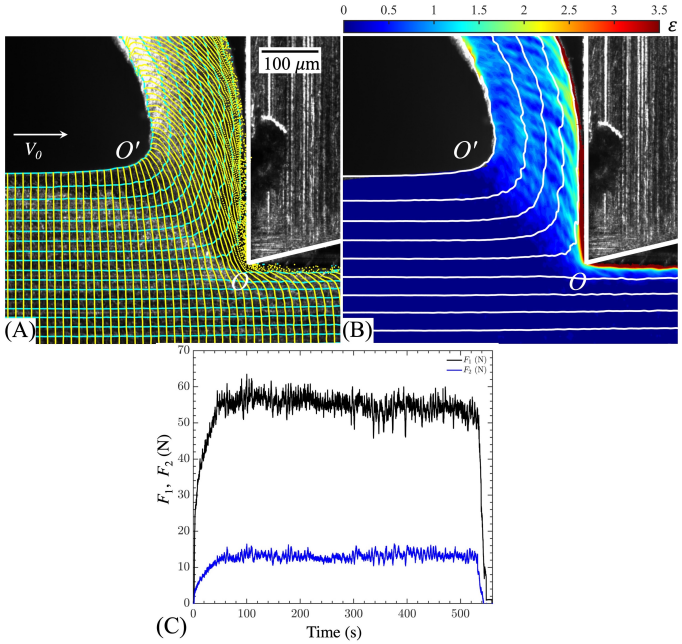

FIGURE 2: CONTINUOUS CHIP (V_0 = 0.05 MM/S). (A) GRID MAP AND (B) EQUIVALENT PLASTIC STRAIN FIELD WITH SUPERIMPOSED STREAKLINES SHOWING UNIFORM DEFORMATION (INSIDE THE CHIP) AND STEADY-STATE MATERIAL FLOW DURING CONTINUOUS CHIP FORMATION. THE STEADY-STATE MATERIAL FLOW IS ALSO REFLECTED IN THE NEARLY CONSTANT FORCE PROFILES SHOWN IN (C). HERE, F_1 AND F_2 ARE THE FORCES ALONG AND PERPENDICULAR TO THE DIRECTION OF V_0.

morphology, see Fig. 3. The deformation pattern of this chip is in stark contrast to the continuous chip. It is characterized by two distinct regions — few microns thick planar shear bands with highly concentrated flow, and trapezoidal segments in between the bands where strain levels are relatively low, about one order lower than the shear band strains. The formation of saw-tooth features is also accompanied by periodic high-amplitude oscillations in the force components (F_1 and F_2).

The dynamics of shear-localized chip formation is illustrated using Fig. 3(A), which shows snapshots of different time instances during formation of a single shear band/segment pair. Similar to Fig. 2(B), the plastic strain field and streaklines are shown superimposed on the actual frames. The time instances of the individual frames are also marked on the corresponding force plot in Fig. 3(B). Frames (a)-(c) in Fig. 3(A) show the shear band nucleation phase. In this phase, a localized strain pocket initiates at the tool tip (see white arrow, frame (a)), which then propagates towards the free surface of the material to establish a thin shear band OO' in frame (c); the shear band strain at this point is about 1.5. As can be also observed from the force plot, both the force components F_1 and F_2 increase monotonically during the shear band nucleation phase, reaching a peak when the band has reached the free surface in frame (c).

As the workpiece further advances against the cutting tool, shear band nucleation is followed by a sliding phase where the chip segment next to the freshly developed shear band "slides" against the workpiece under a dropping load but with a constant

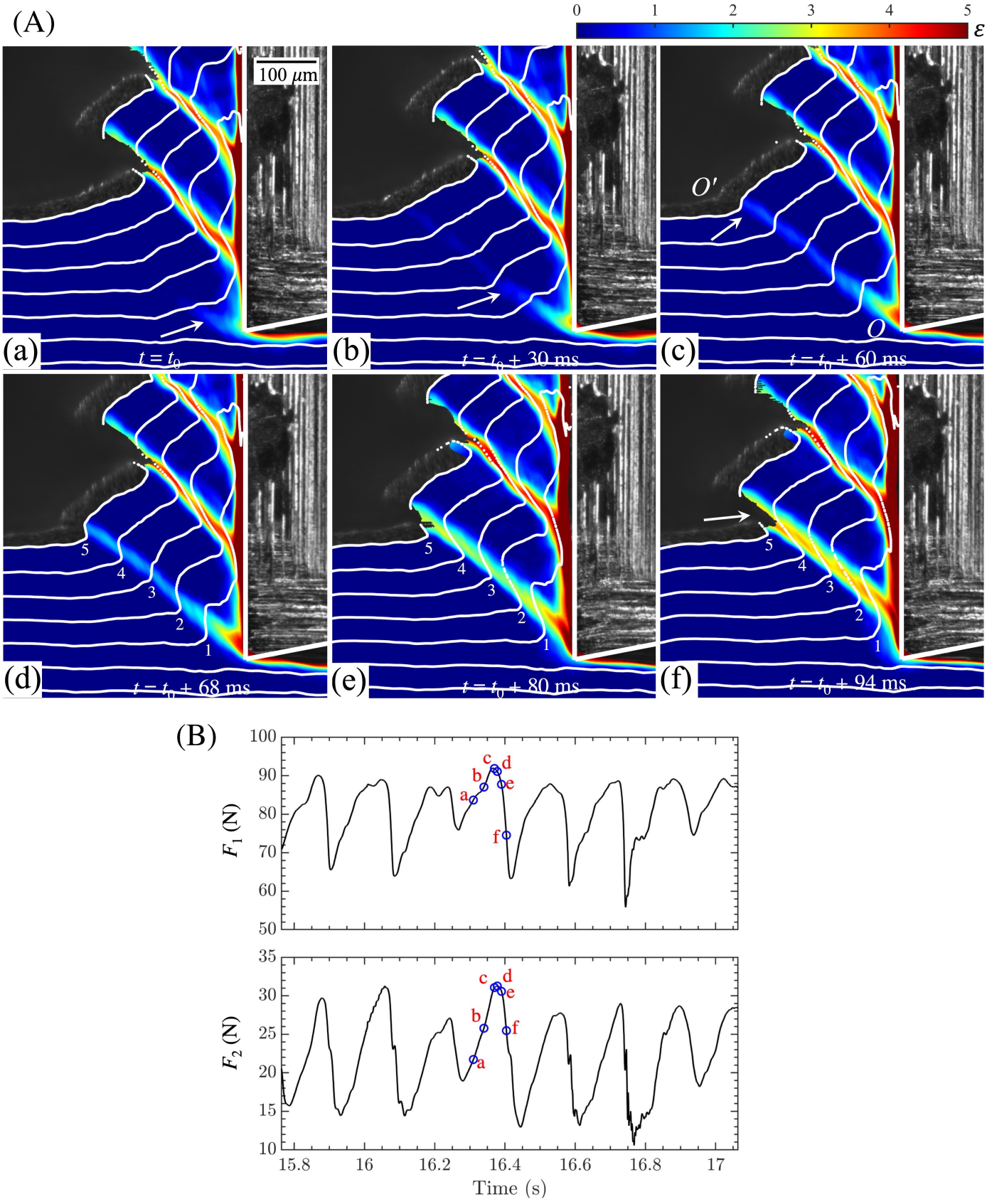

FIGURE 3: SHEAR-LOCALIZED CHIP (V_0 = 1.5 MM/S). (A) HIGH-SPEED IMAGE SEQUENCE WITH SUPERIMPOSED EQUIVALENT PLASTIC STRAIN FIELDS SHOWING SHEAR BAND NUCLEATION (*a–c*) AND SLIDING (*d–f*) PHASES. IN FRAME *a*, A STRAIN INHOMOGENEITY NUCLEATES FROM THE TOOL TIP (SEE ARROW) AND PROPAGATES TOWARDS THE FREE SURFACE RESULTING IN A FULLY DEVELOPED SHEAR BAND *OO′*. FORMATION OF A FULLY DEVELOPED BAND COINCIDES WITH THE PEAK IN THE FORCES, SEE (B). THIS IS FOLLOWED BY SLIDING ALONG THE BAND PLANE, AS SHOWN IN *d–f*, UNDER A DROPPING LOAD. IT IS OBSERVED THAT BOTH THE BAND THICKNESS AND MAGNITUDE OF LOCALIZED STRAIN INCREASE DURING THE SLIDING PHASE.

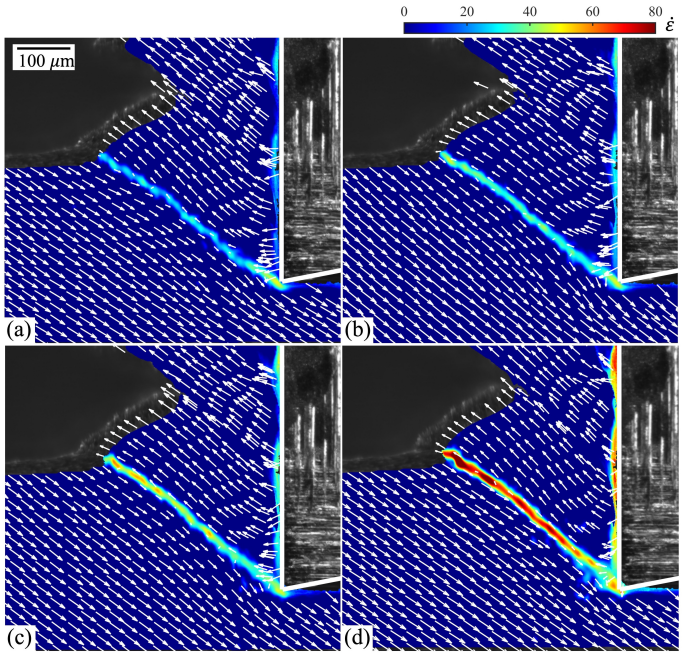

FIGURE 4: EQUIVALENT PLASTIC STRAIN-RATE FIELD DURING THE SHEAR BAND SLIDING PHASE. FRAME *a* CORRESPONDS TO A TIME INSTANCE WHEN THE SHEAR BAND HAS JUST FORMED, WHILE FRAMES *b–d* ARE THOSE TAKEN AT DIFFERENT STAGES OF THE SLIDING PROCESS (SEPARATED BY A TIME INTERVAL OF APPROXIMATELY 6 MS). WHITE ARROWS REPRESENT THE VELOCITY FIELD CALCULATED WITH RESPECT TO THE SHEAR BAND FRAME OF REFERENCE. THE HIGHLY LOCALIZED FLOW WITHIN THE SHEAR BAND AND RIGID-BODY MOTION OF THE MATERIAL ON EITHER SIDE OF THE BAND, WITH EQUAL VELOCITY BUT IN OPPOSITE DIRECTIONS, ARE EVIDENT FROM THE FIGURES. THE EXPERIMENTAL CONDITIONS ARE SAME AS THOSE IN FIG. 3.

velocity V_S. Frames (d)-(f) capture this phase. It is during this phase that most of the strain accumulation happens within the band. For example, it can be seen that the shear band strain increased to about 5 in frame (f) from a strain of 1.5 in frame (c). While sliding takes place under a decreasing load, indicating local weakening of the material in the band, it is important to note that the material remains intact across the shear band. This for example can be seen from the streaklines labeled 1-5 in frames (d)-(f), which undergo stretching as a result of local sliding at the band but remain unbroken. It is only in the local vicinity of the free surface (see arrow in frame (e)) there is some evidence of material separation; as an example, streakline 5 near the free surface shows a discontinuity across the band.

It is also instructive to visualize the sliding phase through the plastic strain-rate fields since the rate field clearly delineates regions of active plastic flow. Figure 4 shows the plastic strain-rate field at four different time instances during the sliding phase. The white arrows (quiver plot), superimposed on the strain-rate fields, show the velocity field with respect to the shear band frame of reference. First, it can be seen that following shear band nucleation in frame (a), the material outside the band is plastically unloaded and the deformation is concentrated only within the band, and a thin secondary shear zone at the tool-chip contact. The strain rate within the band increases initially but stays roughly constant during much of the sliding phase; at the cutting speed (V_0 = 1.5 mm/s) investigated here, the characteristic strain rate within the band is of the order of 10^2 /s. Second, the quiver plots also show that during the sliding phase, the segments on either side of the band essentially slide with respect to each other as rigid bodies in opposite directions with equal velocity. The sliding velocity (V_S) is uniform across the band length, and further analysis shows that V_S is simply the resolved component of V_0 along the band, i.e., $V_S = V_0/\cos(\phi)$, where ϕ is the shear band angle with respect to V_0 direction.

The sliding ceases roughly when F_1 reaches a minimum, and soon after this point, a new shear band nucleates near the tool tip and the cycle repeats in the exact same manner described in frames (a)-(f) of Fig. 3(A). For instance, one may at once observe the similarity between between frame (a), corresponding to shear band nucleation, and frame (f), which represents a time instance near the end of sliding in Fig. 3(A). This cyclic behavior is also evident from the oscillatory force plot in Fig. 3(B), where each cycle corresponds to formation of one shear band/segment pair.

3.3 Fragmented chip

As V_0 is further increased to about 3 mm/s, a second transition in the chip formation mode, from shear-localized chip to fragmented chip, occurs. While the fragmented chip has a similar saw-tooth appearance of a shear-localized chip, the individual segments of the chip are now partially or fully separated from one another due to occurrence of fracture. The high-speed image sequence in Fig. 5(A) illustrates the individual steps involved in the formation of such a chip at V_0 = 4 mm/s. First three frames (a)-(c) show the shear band nucleation phase. As discussed earlier for the shear-localized chip formation, the shear band OO' is established by nucleation of a small strain pocket at the tool tip and its subsequent propagation towards the free surface under an increasing load. However, the next sequence of steps differ considerably from those of the shear-localized chip. Instead of localized sliding along the band, a crack now initiates at the free surface (intersection point of shear band and the workpiece free surface, see arrow in frame (d)) which then propagates closely along the shear band back towards the tool face, see frames (d)-(f). Note that the crack does not propagate all the way till the tool tip but is arrested part-way along the band. This crack propagation along the band, which is accompanied by a load drop (Fig. 5(B)), can be also clearly seen from the streaklines 1-5. As crack propagates with time, these streaklines are broken one-by-one and the segment progressively loses contact with the workpiece. The speed at which crack propagates was found to be $\sim$ 70 mm/s, more than an order of magnitude higher than the cutting speed (V_0 = 4 mm/s); this suggests unstable crack growth.

It is also interesting that with further progress of cutting, crack closure is observed as the next new segment develops under an increasing load. This process is shown in frames (g)-(i). It can be see that the edge of the crack, marked using an arrow in these frames, retraces its path and travels towards the free surface, thus "re-welding" the segments in the process. Note that during crack closure, no strain accumulation takes place along

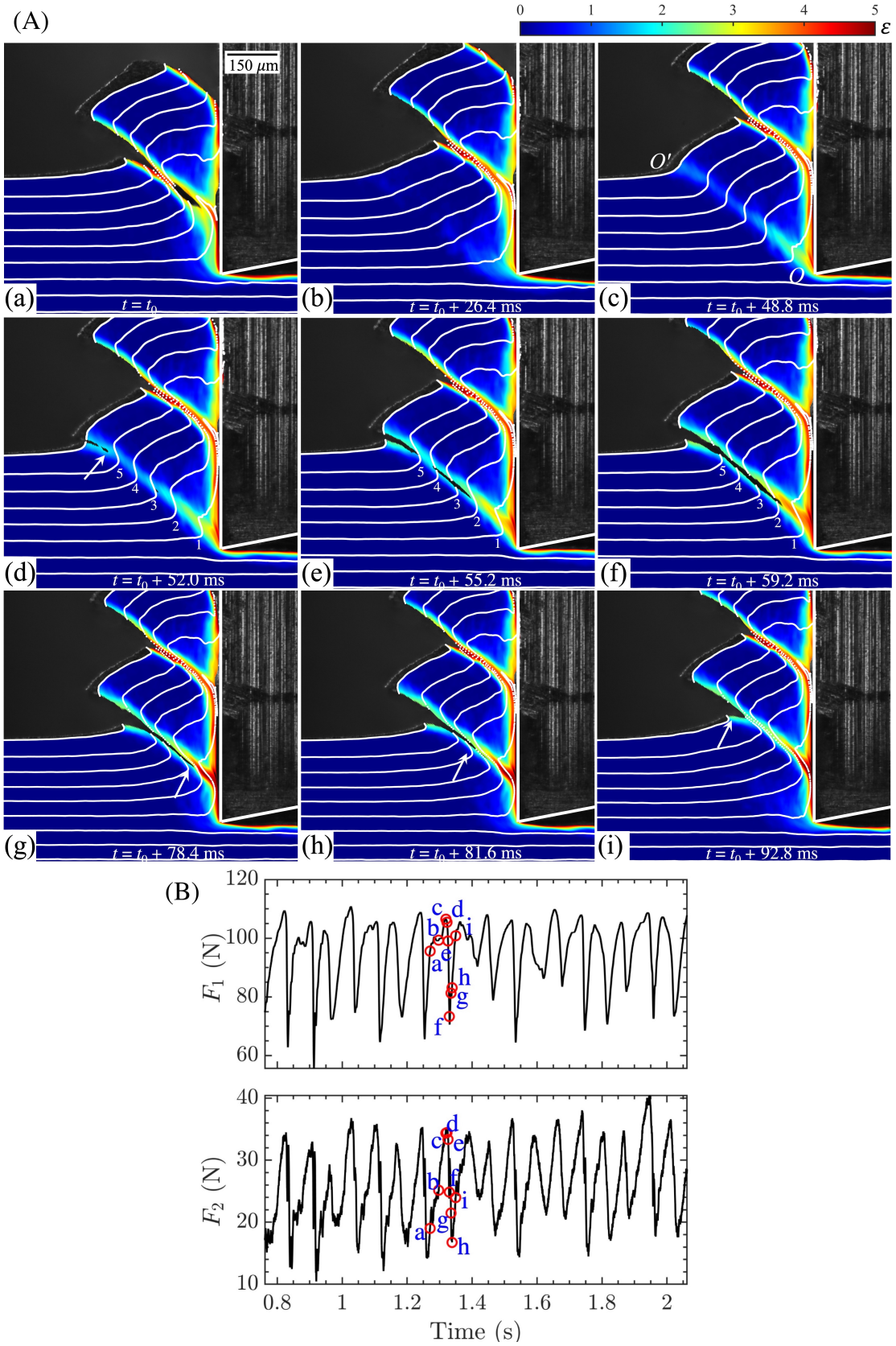

FIGURE 5: PARTIALLY FRAGMENTED CHIP (V_0 = 4 MM/S). (A) HIGH-SPEED IMAGE SEQUENCE, WITH SUPERIMPOSED EQUIVALENT PLASTIC STRAIN FIELD MAPS, SHOWING DIFFERENT STAGES OF CHIP FORMATION PROCESS: SHEAR BAND NUCLEATION (*a–c*), CRACK PROPAGATION (*c–f*), AND CRACK CLOSURE (*g–i*). (B) SHOWS THE CORRESPONDING FORCE PROFILE. FOLLOWING THE SHEAR BAND (*OO′*) FORMATION, A CRACK INITIATES AT THE FREE SURFACE (SEE ARROW, FRAME *d*) AND TRAVELS PART-WAY TOWARDS THE TOOL TIP (FRAMES *e* AND *f*) AS THE LOAD DROPS. THE EXTENT OF CRACK PROPAGATION IN THIS CASE IS ~ 80% OF THE BAND LENGTH. THE STAGE OF CRACK CLOSURE WHICH OCCURS AS THE NEW SEGMENT DEVELOPS UNDER A RISING LOAD IS SHOWN IN FRAMES *g–i*; THE ARROW IN THESE FRAMES SHOW THE POSITION OF THE CRACK EDGE.

the contact as there is no shearing in the segments on either side of the band. The crack closure process concludes roughly when a new shear band nucleates (again at the tool tip) in the freshly formed segment.

Although one can notice a striking similarity in the chip morphology between Fig. 3 and Fig. 5, the basic mechanics of chip formation in both the cases is quite different. While the saw-tooth pattern in shear-localized chip is a direct result of localized sliding (shear) within the band, in the case of fragmented chip, it is a consequence of crack initiation at the surface and its propagation towards the tool. What is common however in both the cases is the shear band nucleation phase (frames (a)-(c) in Figs. 3 and 5). Therefore, shear localization is a *precursor* to fracture and not vice versa.

Figure 6 shows a more extreme case of chip fragmentation at $V_0 = 10$ mm/s, which results in the formation of individual and completely broken segments. As before, the chip formation starts with shear band nucleation (frames (a)-(c)), followed by crack nucleation at the free surface and its back propagation along the band towards the tool, see arrow in frames (d)-(f). However, in contrast to Fig. 5 ($V_0 = 4$ mm/s), the crack now propagates all the way to the tool tip, resulting in complete fragmentation of the segment. The crack speed in this case is also much higher at ~ 200 mm/s, suggesting that crack speed is not a constant but increases with the cutting speed. Rapid crack propagation can be also seen from the plastic strain field in frames (d)-(f), where little strain accumulation is seen in the band after frame (c). Also, unlike the partially fragmented chip seen earlier in Fig. 5, no crack closure was observed in this case and the segments remain completely separated during cutting, see frames (g)-(i).

4. DISCUSSION

In situ imaging of the chip formation process, coupled with PIV analysis, has enabled us to directly capture the transitions between different chip formation modes as a function of the cutting speed as well as characterize the underlying dynamics at high spatial and temporal resolution. The use of a low T_m eutectic alloy in particular allowed different chip formation modes to be reproduced under low cutting speeds (10 mm/s or less), which greatly facilitated direct observations. The study clearly shows how a continuous chip that is characterized by uniform deformation is replaced by a saw-tooth shear-localized chip as V_0 is increased beyond some critical value. The shear-localized chip develops in two distinct phases: shear band nucleation at the tool tip and its propagation towards the free surface to form a thin weak plane (first phase), which is followed by uniform shear along this plane (second phase). It is this shear that results in strain localization in the chip and a saw-tooth pattern. The local shear at the shear band plane occurs at a constant velocity V_S (given by $V_0/\cos(\phi)$), while maintaining physical material continuity across the band; this shows that fracture is not a prerequisite to shear-localized chip formation. As V_0 is further increased, a second transition from shear-localized to fragmented chip occurs. The initial stages of fragmented chip formation, namely band nucleation at the tool tip and its propagation towards the free surface, are identical to that of shear-localized chip. However, localization is now followed by crack nucleation at the free surface, where shear band meets the surface, and subsequent crack propagation closely along the shear band in the direction towards the tool face. The crack travel speed as well as the extent (distance) of crack propagation along the band increase with V_0. Cutting speeds where a crack is arrested part-way along the shear band results in a partially fragmented chip, with individual segments still connected to each other, while crack propagation all the way to the tool face at higher speeds produces a fully fragmented (discontinuous) chip.

These observations provide a unified explanation for how different chips having the same saw-tooth morphology but different deformation characteristics — strain localization without any evidence of cracks vs. strain localization in combination with fracture — are formed depending on the cutting conditions. In this regard, our observations are in direct contrast with the suggestion made by Shaw [16] and Usui [20] that strain localization along a shear band is triggered by crack nucleation at the free surface. Figures 5 and 6 not only show the opposite, that is, shear banding is a *precursor* to crack nucleation, but also reveal that strain localization in fact stops rather than being accentuated when the crack initiates and propagates along the band. Another noteworthy point is the starting location of the crack, namely, free surface, which is resolved in our high-speed imaging observations without any ambiguity. Although *in situ* photography has been employed in some of the earlier studies of discontinuous chip formation, see for example Refs.[10, 21, 29–31], these studies lacked the spatial and temporal resolution required for clearly resolving the crack initiation and propagation. A study that is closest to our observations is that of Nakayama [4], who in his studies of saw-tooth chip formation in cutting of less ductile metals such as hardened steels, presents a case for chip segmentation being triggered by crack nucleation at the free surface of the chip. Our *in situ* observations support Nakayama's conclusion and also further show that the surface location where crack initiates is not arbitrary but is determined by strain localization preceding fracture.

Having developed a coherent picture of how different chip morphologies arise and their dependence on the operating deformation mode (homogeneous flow, shear localization, fracture or a combination thereof), it is of interest to ask what fundamental principles govern the transition between these different deformation modes. Clues to understanding the first transition from homogeneous to shear-localized flow come from our earlier study [25]. As seen from Fig. 3, formation of a thin and well-defined shear band OO' (see frame (c)) coincides with the peak in the cutting force (F_1). This allows us to define a characteristic stresses (τ_C and σ_C) associated with band formation as follows:

$$\tau_C = \frac{F_{shear}}{A_S} = \frac{(F_{1,C}\cos\phi - F_{2,C}\sin\phi)\sin\phi}{bt_0}$$

$$\sigma_C = \frac{F_{norm}}{A_S} = \frac{(F_{1,C}\sin\phi + F_{2,C}\cos\phi)\sin\phi}{bt_0} \qquad (1)$$

In these equations, τ_C and σ_C are the shear and normal stresses acting on the band at the time of its nucleation; $F_{1,C}$ is the peak cutting force (F_1) and $F_{2,C}$ is the value of F_2 at the

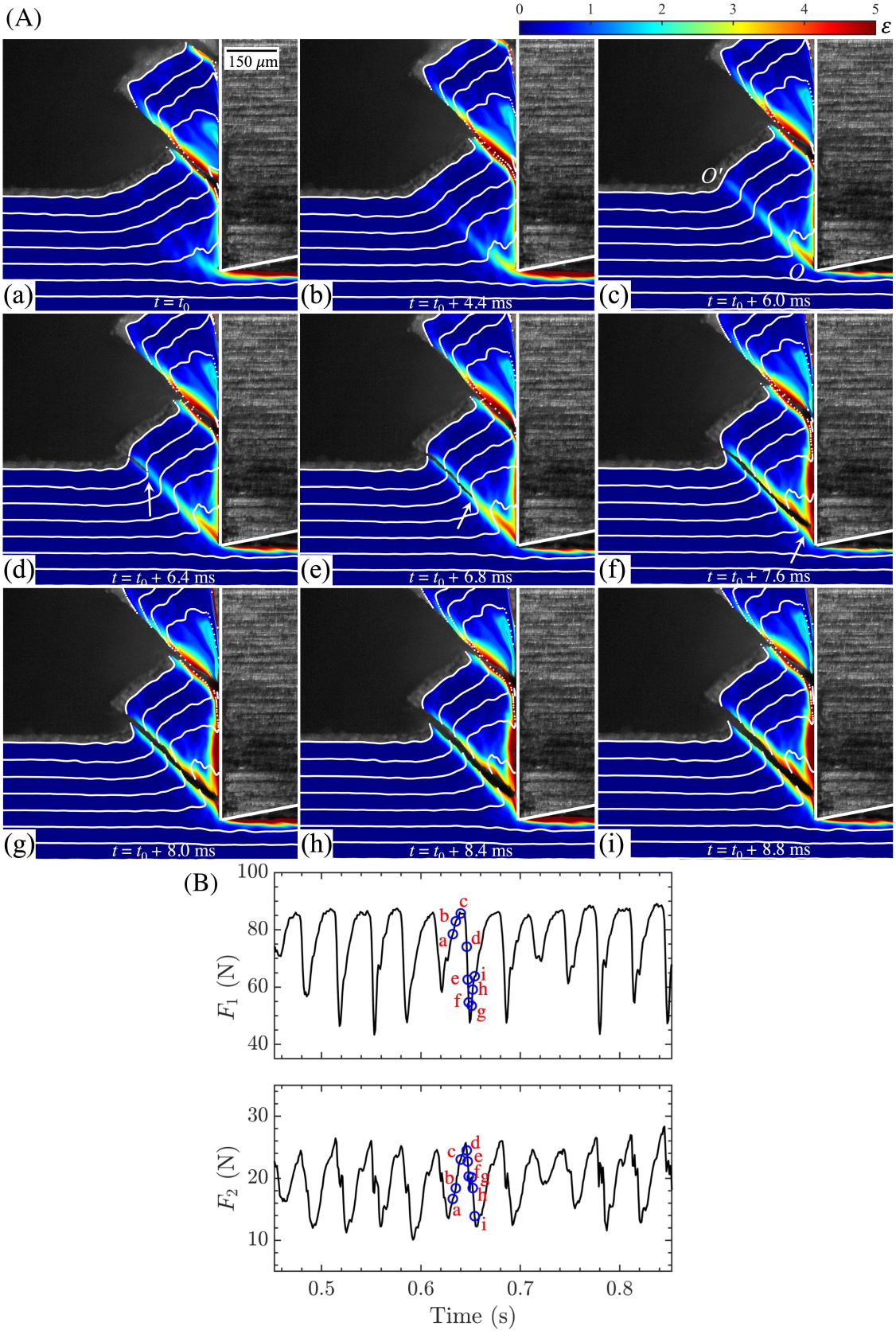

FIGURE 6: FULLY FRAGMENTED (DISCONTINUOUS) CHIP AT V_0 = 10 MM/S, ILLUSTRATED USING HIGH-SPEED IMAGES WITH SUPERIMPOSED PLASTIC STRAIN FIELDS. FRAMES *a–c* IN (A) SHOW SHEAR BAND DEVELOPMENT, WHILE FRAMES *d–f* SHOW THE CRACK NUCLEATION AND PROPAGATION STAGE, WITH THE ARROW SHOWING THE CRACK TIP LOCATION IN EACH FRAME. CRACK TRAVELS ALL THE WAY TO THE TOOL TIP IN THIS CASE, RESULTING IN COMPLETE FRAGMENTATION OF THE CHIP IN FRAME *f*. FRAMES *g–i* SHOW THE DEVELOPMENT OF THE NEXT SEGMENT UNDER AN INCREASING LOAD, SEE FORCE PROFILES IN (B).

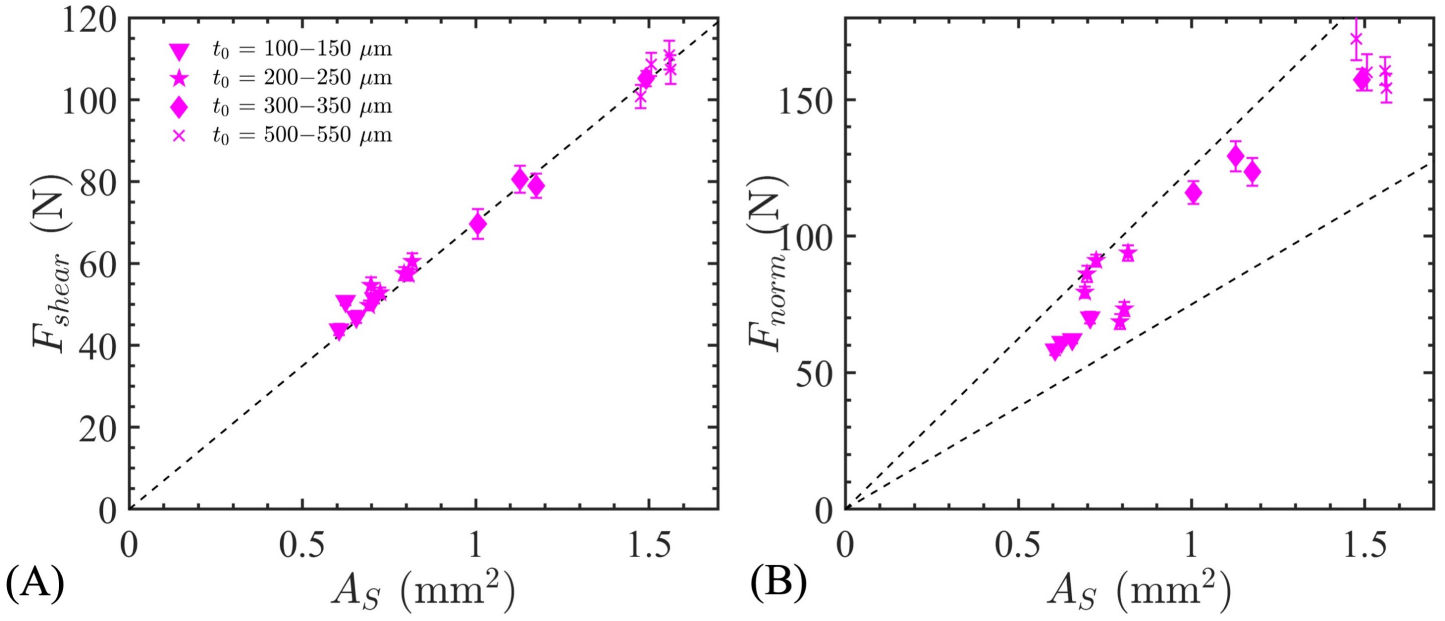

FIGURE 7: PLOTS SHOWING F_{shear} (A) AND F_{norm} (B) DATA PLOTTED AGAINST THE SHEAR BAND AREA (A_S). DATA FROM MULTIPLE CUTTING EXPERIMENTS WITH DIFFERENT t_0 (100 μM TO 550 μM) AND V_0 (1 MM/S TO 10 MM/S). ALL POINTS IN THE F_{shear} VS A_S PLOT FALL ON A STRAIGHT LINE WITH A SLOPE OF ~ 70 MPA, INDICATING THAT THE SHEAR STRESS (τ_C) AT BAND NUCLEATION IS A MATERIAL CONSTANT.

time instance when F_1 reaches a peak; b and t_0 are the cutting width and depth respectively, and ϕ as before is the shear band angle with respect to the V_0 direction. F_{shear} and F_{norm} are the resultant forces acting parallel and normal to the band plane respectively, whereas A_S is the shear band area. Measurements of shear band stresses over different experimental combinations of t_0 and V_0 show that τ_C is a material constant that is independent of the normal stress (σ_C) acting on the band. This is demonstrated in Fig. 7 where F_{shear} and F_{norm} data from different experiments are plotted against the corresponding shear band area (A_S). For each experimental condition, force and area values reported are averages of roughly 200 bands. It is clear from the F_{shear} vs. A_S plot (Fig. 7(A)) that all points fall on a single straight line, given by a slope τ_C of 70 MPa. In contrast, no such line can be drawn for the F_{norm} data in Fig. 1(B). This suggests a critical shear stress-type criterion for shear band formation — that is, when the shear stress is less than τ_C (70 MPa for the Wood's alloy), steady-state homogeneous flow is observed, but when it reaches τ_C, shear band formation sets in and results in highly localized flow.

In fact, experiments with two other low melting point alloys (T_m of 47 °C and 138 °C) have shown that this behavior is not specific to the Wood's alloy but is likely more general. Similar to the Wood's alloy, the onset of shear localization in both of these materials occurred at a critical τ_C that was independent of the normal stress σ_C [25]. Additionally, in all the materials, the ratio of τ_C to the corresponding shear modulus (μ_0) was found to be close to 0.05. This phenomenon is similar to the critical resolved shear stress concept that is commonly used to describe the onset of dislocation slip in metals [32]. The precise microscopic mechanism for shear band formation at a critical shear stress as well as the material-dependence of this stress requires additional study.

Regarding the second transition from shear localization to fracture, two questions arise — why/when does a crack develop, and what controls its propagation speed? Answer to the first question is likely rooted in the competition between two competing processes, localization and fracture, in accommodating the imposed rate. As seen from Figs. 3–6, right after the shear band plane is formed, there are two ways by which further advancement of the workpiece against the tool can be accommodated — by localized shear along the shear band or via propagation of a crack. Localized shear, which involves uniform sliding across the entire band, requires energy of the order of $\tau_C A_S/b$ per unit area extension of the slip. On the other hand, the equivalent energy for the latter is simply the fracture energy required for advancing the crack, which itself decreases with increasing rate in most metals [33, 34]. It is therefore logical to conclude that the observed transition from localized shear to fracture should coincide with the rate (equivalently, V_0) where the fracture energy becomes smaller than the energy needed for uniform plastic shear along the band. Such a picture can also explain the crack speed dependence on V_0 observed in our study. Since the crack velocity depends on the crack extension force [35] — the difference between the elastic energy release rate and fracture energy — crack is expected to travel at a faster speed at higher V_0 because of the lower fracture energy. Verification of this hypothesis however warrants a more quantitative treatment and further high-speed investigations of crack propagation dynamics over a wider range of V_0. These aspects of fracture, as well as the effect of different chip formation modes on the machined surface characteristics, are under current investigation by the authors.

The questions posed above, vis-à-vis onset of shear band instability and its transition to fracture, are in fact part of a wider problem concerning shear fracture, which is a topic of much interested in materials science and solid mechanics. In this context, we believe that cutting configuration, which allows formation of isolated shear bands (i.e., one at a time) at an *apriori* known location (tool tip), offers unique opportunities for direct *in situ* observations of shear fracture over a wide range of strain rates (controlled by V_0). Furthermore, a large number of shear bands can be generated in a single experiment, which should facilitate statistical analysis of fracture attributes such as crack velocity and their dependence on the strain rate. These benefits open new opportunities for using cutting as an innovative experimental tool for studying materials/mechanics phenomena including localization, fracture, size effects and friction (e.g., see Ref. [36]), in addition to its standard machining applications.

5. CONCLUSION

A study has been made of the transitions in the chip formation mode that occur with increasing cutting speed in machining of ductile metals. A low melting point eutectic alloy was used as a model material to reproduce different chip formation modes — continuous chip at lower cutting speeds, followed by a shear-localized chip, and then a fragmented chip at higher speeds. High-speed photography and an image correlation technique, particle image velocimetry, were employed to directly observe the chip formation process *in situ*, quantify the dynamic strain and strain-rate fields, and elucidate various aspects of shear localization and fracture phenomena involved. The principal conclusions are:

- Transition from continuous chip to shear-localized chip beyond a critical cutting speed is triggered by shear band nucleation at the tool edge and its propagation to the free surface. Once a shear band plane is established, further localization within the band occurs by uniform sliding (shear) across the band; the shear steps and saw-tooth pattern at the free surface are also a result of this sliding process.

- Transition from shear-localized to fragmented chip at higher cutting speeds is a result of crack initiation at the surface and its propagation towards the tool tip. In fragmented chip formation, shear localization *precedes* crack initiation, and governs both the surface location of the crack as well as the crack path.

- The extent of crack propagation towards the tool tip governs determines whether the chip is partially fragmented, i.e., with segments still attached to each other, or fully discontinuous. The crack travel speed is about one order of magnitude higher than the cutting speed and increases with increase in the cutting speed.

- Possible mechanisms that govern transitions between different chip formation modes are outlined. It is shown that a critical shear stress criterion describes the first transition, while the second transition most likely arises from relative competition between plastic shear and fracture within a shear band.

Future work will explore the generality of our experimental observations over a broader range of material systems and cutting speeds.

ACKNOWLEDGMENTS

The work was supported by the US National Science Foundation through grant no. CMMI-2102030; and the TAMUS National Laboratories Office (NLO) Los Alamos National Laboratory (LANL) Collaborative Research Program through award no. CF5789.

REFERENCES

[1] Shaw, M. C. *Metal Cutting Principles*. Oxford University Press, Oxford, UK (1989).

[2] Sagapuram, D., Udupa, A., Viswanathan, K., Mann, J. B., M'Saoubi, R., Sugihara, T. and Chandrasekar, S. "On the cutting of metals: A mechanics viewpoint." *Journal of Manufacturing Science and Engineering* Vol. 142 No. 11 (2020): p. 110808.

[3] Yeung, H., Viswanathan, K., Compton, W. D. and Chandrasekar, S. "Sinuous flow in metals." *Proceedings of the National Academy of Sciences* Vol. 112 No. 32 (2015): pp. 9828–9832.

[4] Nakayama, K. "On the formation of "saw-toothed chip" in metal cutting." *Journal of the Japan Society for Precision Engineering* Vol. 43 (1977): pp. 117–122.

[5] Guo, Y., Compton, W. D. and Chandrasekar, S. "*In situ* analysis of flow dynamics and deformation fields in cutting and sliding of metals." *Proceedings of the Royal Society A: Mathematical, Physical and Engineering Sciences* Vol. 471 No. 2178 (2015): p. 20150194.

[6] Recht, R. F. "Catastrophic thermoplastic shear." *Journal of Applied Mechanics* Vol. 31 No. 2 (1964): pp. 186–193.

[7] Komanduri, R. "Machining and grinding: A historical review of the classical papers." *Applied Mechanics Reviews* Vol. 46 No. 3 (1993): pp. 80–132.

[8] Viswanathan, K., Yadav, S. and Sagapuram, D. "Shear bands in materials processing: Understanding the mechanics of flow localization from Zener's time to the present." *Applied Mechanics Reviews* Vol. 72 No. 6 (2020): p. 060802.

[9] Fazlali, M. and Jin, X. "Time-Varying Tool-Chip Contact in the Cutting Mechanics of Shear Localization." *Journal of Manufacturing Science and Engineering* (2023): pp. 1–24.

[10] Field, M. and Merchant, M. E. "Mechanics of formation of the discontinuous chip in metal cutting." *Transactions of the American Society of Mechanical Engineers* Vol. 71 No. 5 (1949): pp. 421–428.

[11] Cook, N. H., Finnie, I. and Shaw, M. C. "Discontinuous chip formation." *Transactions of the American Society of Mechanical Engineers* Vol. 76 No. 2 (1954): pp. 153–162.

[12] Flom, D. G., Komanduri, R. and Lee, M. "High-speed machining of metals." *Annual Review of Materials Science* Vol. 14 No. 1 (1984): pp. 231–278.

[13] Komanduri, R. and Schroeder, T. A. "On shear instability in machining a nickel-iron base superalloy." *Journal of*

Engineering for Industry Vol. 108 No. 2 (1986): pp. 93–100.

[14] Gente, A., Hoffmeister, H. W. and Evans, C. J. "Chip formation in machining Ti6Al4V at extremely high cutting speeds." *CIRP Annals* Vol. 50 No. 1 (2001): pp. 49–52.

[15] Barry, J. and Byrne, G. "The Mechanisms of Chip Formation in Machining Hardened Steels." *Journal of Manufacturing Science and Engineering* Vol. 124 No. 3 (2002): pp. 528–535.

[16] Shaw, M. C. and Vyas, A. "Chip formation in the machining of hardened steel." *CIRP Annals* Vol. 42 No. 1 (1993): pp. 29–33.

[17] Sagapuram, D., Viswanathan, K., Trumble, K. P. and Chandrasekar, S. "A common mechanism for evolution of single shear bands in large-strain deformation of metals." *Philosophical Magazine* Vol. 98 No. 36 (2018): pp. 3267–3299.

[18] Komanduri, R. and Von Turkovich, B. F. "New observations on the mechanism of chip formation when machining titanium alloys." *Wear* Vol. 69 No. 2 (1981): pp. 179–188.

[19] Turley, D. M., Doyle, E. D. and Ramalingam, S. "Calculation of shear strains in chip formation in titanium." *Materials Science and Engineering* Vol. 55 No. 1 (1982): pp. 45–48. DOI https://doi.org/10.1016/0025-5416(82)90082-9. URL https://www.sciencedirect.com/science/article/pii/0025541682900829.

[20] Usui, E., Obikawa, T. and Shirakashi, T. "Study on chip segmentation in machining titanium alloy." *Proceedings of the 5th International Conference on Producting Engineering Tokyo*. 1984.

[21] Ho, W. S. and Brewer, R. C. "A slip-line field solution for machining with discontinuous chips." *Proceedings of the Institution of Mechanical Engineers* Vol. 180 No. 1 (1965): pp. 791–802.

[22] Obikawa, T., Sasahara, H., Shirakashi, T. and Usui, E. "Application of computational machining method to discontinuous chip formation." *Journal of Manufacturing Science and Engineering* Vol. 119 No. 4B (1997): pp. 667–674.

[23] Yadav, S., Feng, G. and Sagapuram, D. "Dynamics of shear band instabilities in cutting of metals." *CIRP Annals* Vol. 68 (2019): pp. 45–48.

[24] Yadav, S. and Sagapuram, D. "*In situ* analysis of shear bands and boundary layer formation in metals." *Proceedings of the Royal Society A: Mathematical, Physical and Engineering Sciences* Vol. 476 No. 2234 (2020): p. 20190519.

[25] Yadav, S. and Sagapuram, D. "Nucleation properties of isolated shear bands." *Proceedings of the Royal Society A* Vol. 476 No. 2241 (2020): p. 20200529.

[26] Adrian, R. J. and Westerweel, J. *Particle Image Velocimetry*. Cambridge University Press (2010).

[27] Chawla, H., Yadav, S., Aprahamian, H. and Sagapuram, D. "Determining large-strain metal plasticity parameters using in situ measurements of plastic flow past a wedge." *Proceedings of the Royal Society A* Vol. 479 No. 2275 (2023): p. 20230061.

[28] Merchant, M. E. "Mechanics of the metal cutting process. I. Orthogonal cutting and a type 2 chip." *Journal of Applied Physics* Vol. 16 No. 5 (1945): pp. 267–275.

[29] Salmon, R., Rice, W. B. and Russel, L. T. "Force variation during the formation of continuous segmented chips in metal cutting." *Canadian Journal of Engineering* Vol. 45 (1962): p. 59.

[30] Enahoro, H. E. and Oxley, P. L. B. "An investigation of the transition from a continuous to a discontinuous chip in orthogonal machining." *International Journal of Mechanical Sciences* Vol. 3 No. 3 (1961): pp. 145–156.

[31] Gane, N. "The effect of lead on the friction and machining of brass." *Philosophical Magazine A* Vol. 43 No. 3 (1981): pp. 545–566.

[32] Cottrell, AH. *Dislocations and Plastic Flow in Crystals*. Oxford University Press, New York (1953).

[33] Zener, C. "The micro-mechanism of fracture." Jonassen, F., Roop, W.P. and Bayless, R.T. (eds.). *Fracturing of Metals*. American Society for Metals, Cleveland, Ohio (1948): pp. 3–31.

[34] Ravi-Chandar, K. *Dynamic Fracture*. Elsevier (2004).

[35] Maugis, D. *Contact, Adhesion and Rupture of Elastic Solids*. Vol. 130. Springer Science & Business Media (2000).

[36] Feng, G. and Sagapuram, D. "A strong basis for friction as the origin of size effect in cutting of metals." *International Journal of Machine Tools and Manufacture* Vol. 168 (2021): p. 103741.